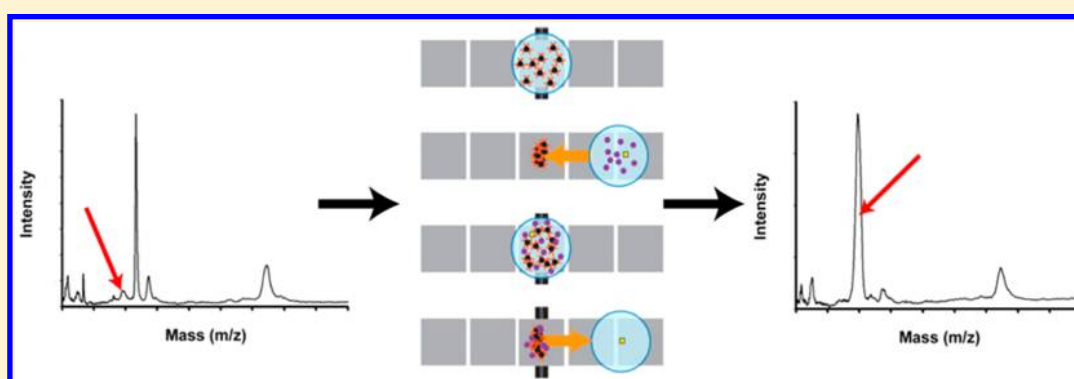


Digital Microfluidic Platform for Human Plasma Protein Depletion

Ningsi Mei,^{†,||} Brendon Seale,^{‡,||} Alphonsus H.C. Ng,^{§,⊥} Aaron R. Wheeler,^{*,‡,§,⊥} and Richard Oleschuk^{*,†}[†]Department of Chemistry, Queen's University, 90 Bader Lane, Kingston, Ontario K7L 3N6, Canada[‡]Department of Chemistry, University of Toronto, 80 St. George Street, Toronto, Ontario M5S 3H6, Canada[§]Institute of Biomaterials and Biomedical Engineering, University of Toronto, 164 College Street, Toronto, Ontario M5S 3G9, Canada[⊥]Donnelly Centre for Cellular and Biomolecular Research, 160 College Street, Toronto, Ontario M5S 3E1, Canada

Supporting Information



ABSTRACT: Many important biomarkers for disease diagnosis are present at low concentrations in human serum. These biomarkers are masked in proteomic analysis by highly abundant proteins such as human serum albumin (HSA) and immunoglobulins (IgGs) which account for up to 80% of the total protein content of serum. Traditional depletion methods using macro-scale LC-columns for highly abundant proteins involve slow separations which impart considerable dilution to the samples. Furthermore, most techniques lack the ability to process multiple samples simultaneously. We present a method of protein depletion using superparamagnetic beads coated in anti-HSA, Protein A, and Protein G, manipulated by digital microfluidics (DMF). The depletion process was capable of up to 95% protein depletion efficiency for IgG and HSA in 10 min for four samples simultaneously, which resulted in an approximately 4-fold increase in signal-to-noise ratio in MALDI-MS analysis for a low abundance protein, hemopexin. This rapid and automated method has the potential to greatly improve the process of biomarker identification.

Recently, clinical proteomics has emerged as an important field for the discovery of disease biomarkers. In particular, researchers are now systematically searching the human plasma proteome for biomarkers that can be used to predict the risk of cancer or monitor the progression of disease.¹ However, these efforts are hindered by the complexity of plasma, which has a proteome that spans 10 orders of magnitude in concentration.² As such, biomarkers at low concentrations can be masked by highly abundant proteins (HAPs) such as immunoglobulins (Igs) and human serum albumin (HSA).^{3,4}

To reduce the complexity of plasma, many proteomic workflows include a pretreatment procedure that depletes HAPs from the sample.^{5,6} These depletion procedures typically use affinity chromatography spin columns, which contain affinity ligands that bind to specific HAPs to remove them from the sample.^{7–13} Although affinity chromatography is a useful pretreatment strategy, there are drawbacks that limit its effectiveness. First, chromatography is a labor intensive process, requiring many sample preparation steps (e.g., multiple fluid

handling steps followed by centrifugation). Additionally, the depletion process requires at least a 10-fold dilution of the sample in an appropriate loading buffer.¹⁴ Furthermore, there is a risk of sample loss arising from protein degradation during the long pretreatment procedure (30 min to 2 h), postextraction concentration steps to counteract the sample dilution, and sample handling during transfer and aspiration. These limitations represent both a major source of variability and a bottleneck for clinical proteomics.

To address these limitations, some groups have explored the concept of miniaturizing affinity chromatography using microfluidics.^{15–17} Microfluidic affinity chromatography has the potential to speed up protein depletion, minimize sample dilution, and eliminate the need for centrifugation and trained personnel. In a recent example, McKenzie et al.¹⁸ demonstrated

Received: June 16, 2014

Accepted: July 24, 2014

Published: July 24, 2014

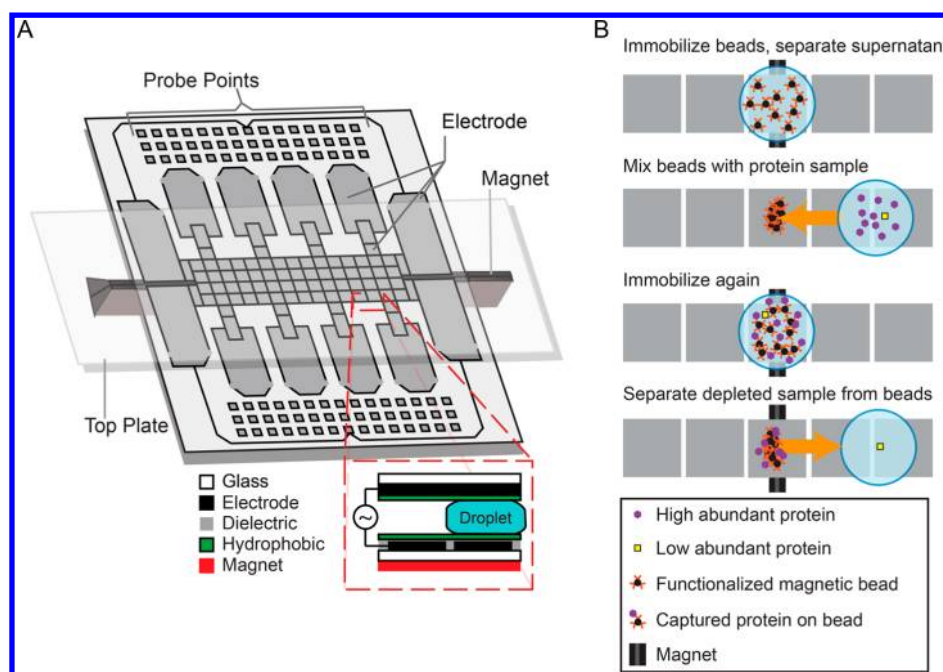


Figure 1. Device and processing scheme. (A) Schematic representation of the digital microfluidic device used for protein depletion in the automated magnetic separation system. Inset shows a cross-section of the device layers when the magnet is in position for magnetic separation. (B) Schematic representation of protein depletion using magnetic beads and digital microfluidics. First, functionalized magnetic beads are isolated from their supernatant by magnetic separation. Second, protein samples are added to the magnetic beads and mixed. Third, application of a magnetic field immobilizes the beads again. Fourth, the immobilized beads are separated from the depleted protein solution by DMF actuation, and the depleted sample is ready for analysis.

a pneumatically driven microfluidic device that depletes 66–77% of immunoglobulins (IgGs) from a complex sample using Protein G functionalized beads dried on the device surface. The work was focused on preventing false positives in IgM assays and did not examine proteomic sample preparation. In parallel, many groups have developed microfluidic systems to conduct immunoassays.¹⁹ Analogous analyte capture concepts developed for microfluidic immunoassays can be similarly applied to HAP depletion, the difference being that, in immunoassays, the unbound constituents are discarded, while in HAP depletion, the unbound constituents are preserved.

Several liquid actuation schemes have been explored for microfluidics;²⁰ however, digital microfluidics (DMF) has a number of potential advantages for HAP depletion. In DMF, discrete droplets are manipulated by electrostatic forces on an array of electrodes coated with a hydrophobic insulator.²¹ When a sequence of voltages is applied to the electrodes, droplets can be addressed individually and made to move, merge, mix, and dispense from sample/reagent reservoirs.²² Since droplet operations can be conveniently controlled, experimental conditions can be modified to alter the protein depletion time or implement multistage depletion using the same device design.^{5,23,24} DMF has been used in several sample preparation/extraction strategies, including protein precipitation,²⁵ reversed-phase²⁶ and strong cation exchange²⁷ solid-phase extraction, and liquid–liquid extraction.^{28,29} In addition, DMF has been implemented for magnetic bead-based immunoassays,^{30–33} in which an external magnet facilitates the separation of droplets from antibody-coated beads. To our knowledge, DMF has never been used as a proteomic preparation tool for HAP depletion.

We report here the development of a new protein depletion platform that relies on DMF for liquid handling and superparamagnetic beads (coated with Protein A, Protein G,

and Anti-HSA antibodies) for removal of abundant proteins. This new device brings about enhancements to traditional chromatography spin columns or flow-based microfluidic platforms. First, this method is fully automated and does not require external agitation for mixing or centrifugation; after placing the sample in the device, no further manual intervention is required. Second, the device depletes proteins rapidly because of efficient bead/sample mixing during incubation³¹ (e.g., ~9 min is required to remove 95% of a 0.5 mg/mL protein from solution). Third, the device can be programmed to carry out various permutations of protein depletion, involving the simultaneous or sequential removal of HSA and IgG. Finally, we propose that this has the potential for facile integration with other microfluidic proteomic processing techniques including reduction, alkylation, and digestion^{34,35} and separations.³⁶

EXPERIMENTAL SECTION

Reagents and Materials. Unless otherwise noted, reagents were purchased from Sigma-Aldrich (Oakville, ON). Deionized water (DI H₂O) was utilized for all solution preparation and had a resistivity of >18 MΩ·cm at 25 °C. All protein and processing reagent solutions were prepared in working buffer (aqueous phosphate buffered saline, PBS, containing 1.5 mM KH₂PO₄, 155 mM NaCl, and 2.7 mM Na₂HPO₄ at pH 7.2, supplemented with 0.05% w/v Pluronic F-68) prior to use.

On-Chip Protein Depletion Reagents. Reagents used on-chip were prepared in-house. Protein solutions of human serum albumin (HSA, molecular weight based on amino acid composition of 66 437 Da) and hemopexin (molecular weight approximately 57 000 Da), were formed from lyophilized solid in PBS buffer, purchased from Life Technologies (Carlsbad, CA). Solutions of human IgG (molecular weight approximately 150 000 Da) were diluted from a stock solution of 4.7 mg/mL in

PBS buffer. Superparamagnetic beads with specific functional coatings were obtained from Millipore (Billerica, MA). For the depletion of IgG and HSA, PureProteome Protein A/G Mix Magnetic Beads (LSKMAGAG02) and PureProteome Albumin Magnetic Beads (LSKMAGL02) were used, respectively. The beads are 10 μm in diameter and are coated with a mix of Proteins A and G and anti-HSA, respectively. Bead dilutions were performed by immobilizing the beads in a magnetic separation rack, removing the supernatant, and adding the desired volume of PBS. Two types of suspensions were used here: Protein A/G beads alone (at a dilution of 1:4 from stock) or a mixture of Protein A/G beads (at a dilution of 1:4 from stock) and anti-HSA beads (at a dilution of 1:2 from stock). Magnetic bead concentrations were determined using capacity values from the supplier. Fluorescein-isothiocyanate (FITC) labeled human IgG at 0.5 mg/mL was purchased from GenScript USA Inc. (Piscataway, NJ). FITC labeled HSA at 1 mg/mL was purchased from Abcam (Cambridge, MA).

Off-Chip MALDI and LC-MS/MS Protein Depletion Analysis Reagents.

ZipTip C4 pipet tips and Milli-Q water were purchased from Millipore (Etobicoke, ON). MALDI matrix solution was prepared by dissolving 10 mg of sinapinic acid (SA) in 1 mL of 50:50 DI H_2O /acetonitrile (ACN) obtained from Caledon (Georgetown, ON) containing 0.1% trifluoroacetic acid (TFA) from Thermo Scientific Pierce (Nepean, Ontario). Bovine serum albumin (BSA) obtained from Mann Research Laboratories (Port Saint Lucie, FL, USA) was used as the calibration standard for the analysis of all samples.

Device Fabrication and Operation. Digital microfluidic devices were fabricated in the University of Toronto Nanofabrication Centre (TNFC) clean room facility and were assembled as described previously (Figure 1A),³⁰ for details, see the Supporting Information. An automated two plate actuation system (described in detail elsewhere³¹) was used to control droplet movement and magnet position for the immobilization of magnetic particles. Droplet movement is controlled via custom Microdrop³⁷ software which was interfaced to the control system to engage a magnetic lens assembly. This magnet provides approximately 600 μN of force which exceeds the minimal threshold for magnetic separation (470 μN).³¹ Droplet driving voltages were between 100 and 120 V_{RMS} at 10 kHz (sine wave). During incubation, the droplets were moved in a modified “figure 8” pattern (Video S1, Supporting Information) to ensure proper dispersal of particles. Waste and unused fluids were removed from devices by wicking using KimWipes (Kimberly-Clark, Irving, TX).

On-Chip Protein Depletion Protocol. On-chip protein depletion was performed in eight steps: (1) One droplet each of superparamagnetic magnetic beads and protein sample (4 μL each) were loaded on the device, (2) beads were actuated into the device array, (3) the magnet was engaged to immobilize the beads onto the device surface, (4) the supernatant was removed from the beads, (5) the protein sample droplet was merged with the beads and the beads were dispersed, (6) the suspension was actively incubated (moved in a figure 8 pattern, as above) for 10 min, (7) the beads were immobilized and the supernatant was separated from the beads, and (8) the depleted protein sample droplet was collected in the reservoir for removal and subsequent analysis (2 min). In practice, the eight-step procedure was typically performed on four protein samples in parallel.

Fluorescent Characterization of On-Chip Depletion.

The kinetics of on-chip depletion was probed using FITC-IgG and a suspension of Protein A/G beads, using a variation of the protocol described above. Briefly, steps (1–5) were applied to a sample of FITC-IgG (0.5 mg/mL), which was then incubated for only 30 s in step (6). After steps (7–8), the supernatant droplet was driven to an unused portion of the device, and the fluorescence intensity was probed by loading the device into a plate reader (PHERAstar microplate reader, BMG Labtech, Ortenberg, Germany). Measurements were performed in “well scanning mode” (COSTAR 96 well plate geometry) with three flashes per scan point and a gain of 100 using 485 nm excitation and 520 nm emission. After measurement, the depletion was continued by resuspending the beads in the FITC-IgG droplet and mixing for an additional 30 s, followed by extracting the supernatant (steps 5–8) for another measurement of fluorescence. This procedure (deplete for 30 s, extract supernatant, measure fluorescence, and resuspend beads) was repeated until 10 min of total incubation time was completed.

The efficiency of on-chip depletion of both IgG and HSA was tested using a suspension of Protein A/G and anti-HSA beads. The two analytes were evaluated separately. For IgG, a droplet of 0.5 mg/mL FITC-IgG was extracted (steps 1–8) with active incubation for 10 min in step (6). In step (8), the supernatant droplet was driven to an unused portion of the device, and the fluorescence intensity was probed as above. The supernatant droplet was then extracted again (steps 1–8) using a fresh aliquot of beads, followed by a second fluorescence intensity measurement. For HSA, an identical process was used to extract 0.5 mg/mL FITC-HSA, except with a gain of 125 in the fluorescence intensity measurements. For all fluorescence experiments, the intensity data were normalized to the control intensity (before depletion) to obtain relative values. Fluorescence measurements were carried out on three to four samples with fluorescence determined for each sample following 10 min depletions. Blank measurements were taken from on-chip regions with no droplets.

MALDI-MS Characterization of On-Chip Depletion.

Protein mixture solutions containing two high-abundance proteins (2 mg/mL human IgG and 0.5 mg/mL HSA) and one low-abundance protein (0.1 mg/mL hemopexin) were depleted by digital microfluidics as described above. Samples were collected for MALDI-MS analysis before depletion, after a single round of depletion with one aliquot of mixed beads, and after two rounds of depletion with two aliquots of mixed beads. Depleted samples were collected for analysis by removing the top plate and transferring the sample droplet by pipet. Four replicates were collected and evaluated for each single and double depletion experiment.

After processing by DMF, each sample was purified using a ZipTip C4 according to the manufacturer's instructions. Briefly, ZipTip C4 tips were wetted in 50% ACN containing 0.1% TFA (5 \times) and then equilibrated in 0.1% TFA (5 \times). After equilibrating, fluid in the ZipTip C4 pipet tips was drawn in and out of the tip for 20 cycles for a maximum binding of complex mixtures and then washed with 0.1% TFA (3 \times). Finally, samples were eluted directly in SA matrix solution onto a stainless steel MALDI target plate. After drying, spots were analyzed using a PerSeptive Biosystems Voyager DE Pro MALDI-TOF Mass Spectrometer (AB Sciex, Framingham, MA, USA) operating over a m/z range of 20 000–200 000. A total of 250 shots were collected per spectrum, with laser power adjusted to optimize the signal-to-noise ratio (S/N). Data were

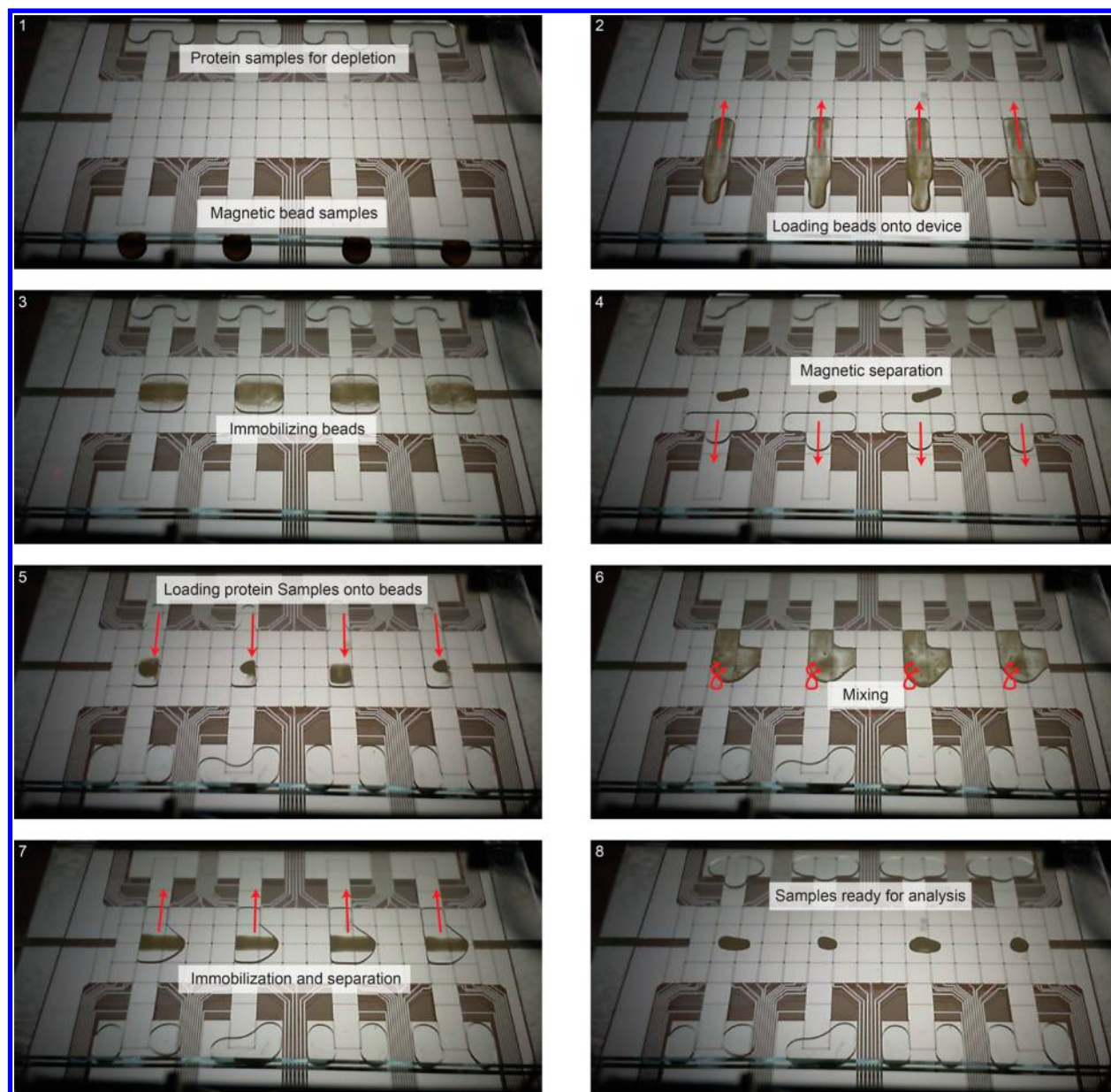


Figure 2. Frames from a video depicting the process of protein depletion (the video is available in the Supporting Information). The dark areas on the array are the magnetic beads.

processed by baseline correction, resolution (set to 100), and noise smoothed (default settings) using Voyager Data Explorer software. Signals were extracted from prominent peak heights, and root-mean square noise (N_{RMS}) values were estimated from a spectra region with no prominent peaks (m/z 88 000–120 000).

RESULTS AND DISCUSSION

DMF Device and Method. Digital microfluidics enables the manipulation of discrete droplets on an array of electrodes and thus offers a number of advantages for sample preparation prior to biochemical analysis. We hypothesized that digital microfluidics would be a convenient platform to use for depletion of HAPs from complex proteomic samples. Current commercially available depletion methods for depletion of a single protein on columns such as the ProtoPrep 20 (Sigma-Aldrich)⁴² require between 20 and 60 min for completion for a single sample. The

device used here is shown in Figure 1A. Droplets of samples and reagents are loaded into reservoir electrodes, where they can be aliquoted/dispensed, mixed, and separated using a defined voltage program. In addition to droplet manipulation, samples can be further manipulated using antibody-functionalized superparamagnetic particles. The particles can be controlled with magnetic fields, allowing for separation of specific molecules bound to the particles from the remainder of the droplet (the “supernatant”). The interplay between magnetic forces and interfacial forces arising from droplet manipulation can be tuned by moving a magnet vertically under the device³¹ (either close to the device, “engaged”, or away from the device, “disengaged”).

A general scheme for HAP depletion by DMF and magnetic particle immobilization is depicted in Figure 1B. As shown, a droplet containing superparamagnetic particles is positioned over an engaged magnet, the initial supernatant is driven away, and a second droplet containing proteomic analytes is delivered

to the immobilized beads. The magnet is then disengaged allowing for resuspension of the particles and active mixing, followed by engaging the magnet a second time to allow for the particles to be separated again. The resulting supernatant droplet should (ideally) contain substantially depleted concentrations of constituents that are bound to the beads. The full process is shown in Figure 2, which depicts a series of images from a movie (available in the Supporting Information). With the device format used here, it was feasible to implement this process in a multiplexed fashion, up to four samples at a time. With the recent report of DMF devices bearing thousands of independently addressable electrodes,³⁸ we propose that, in the future, much higher levels of multiplexing might be achieved.

On-Chip Depletion Kinetics and Efficacy. Two fluorescent assays were developed to determine appropriate conditions for protein depletion. First, an assay to determine the kinetics of depletion was developed, using fluorescently labeled IgG (FITC-IgG) and Protein A/G-labeled particles (Proteins A and G bind IgG with high specificity). Supernatant droplets containing FITC-IgG were probed repeatedly after successive 30 s incubations with particles using techniques reported previously^{5,23,24} for on-chip fluorescence analysis. Figure 3A shows the trend observed for the relative fluorescence intensity as a function of increased contact time with the Protein A/G beads. The fluorescence intensity initially decreases rapidly but gradually stabilizes after 5 min of exposure to the superparamagnetic particles. Following 9 min of exposure, the fluorescence intensity is reduced by >95%, and further depletion time did not result in a substantial fluorescence intensity reduction. As a result, we established a conservative mixing/contact time of 10 min for subsequent depletion experiments.

The second assay was developed to evaluate the depletion efficacy for the two most prevalent HAPs in human serum: IgG (again monitored as FITC-IgG) and HSA (monitored as FITC-HSA), with a mixture of particles bearing Protein A/G (for IgG) and anti-HSA (for HSA). In practice (as described below), the two proteins can be depleted simultaneously, but for this assay, because the same fluorophore was used for both analytes, they were probed sequentially. As shown in Figure 3B, the relative fluorescence intensity decreased dramatically after a single depletion, with >95% reduction following 10 min of contact. A second depletion step was then studied to explore whether the fluorescent intensity could be reduced further. A second aliquot of functionalized superparamagnetic particles was actuated to the center of the chip and mixed with the sample for an additional 10 min. The second depletion resulted in a further reduction of fluorescence intensity, 98% relative to the initial fluorescence intensities. In the future, if different concentrations of proteins or densities of particles are used, it may be useful to evaluate additional (sequential) depletions. Regardless, the depletion efficiencies shown in Figure 3B are similar to those of commercially available extraction methods which remove $\approx 98\%$ of the high abundance proteins.³⁹

MALDI-MS Analysis of DMF-Based Protein Depletion. Fluorescence measurements provide a quantitative assessment of the amount of a high abundance protein that is removed following a single and double depletion steps, but little information is obtained regarding the specificity of the superparamagnetic particle-based depletion process. Off-chip MALDI-MS analysis was used to evaluate the specificity and detection enhancement afforded through superparamagnetic particle/DMF-based protein depletion. MALDI-MS has been used as a semiquantitative profiling tool for proteomic

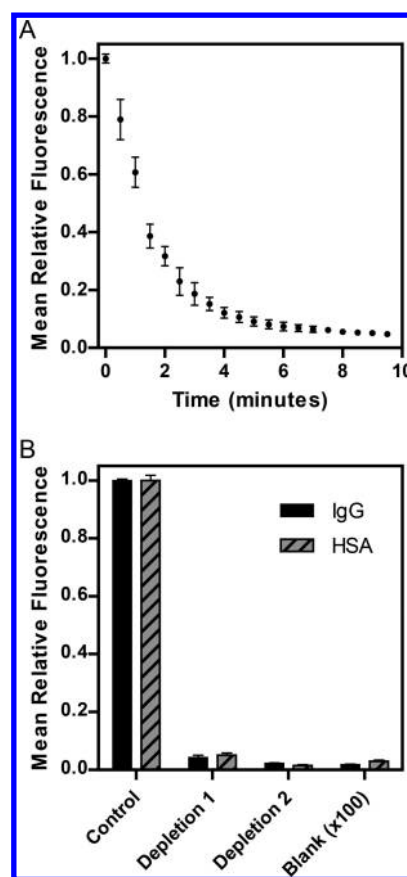


Figure 3. On-chip depletion kinetics and efficacy. (A) Graph of mean relative FITC-IgG fluorescence intensity (normalized to $t = 0$) as a function of mixing time using Protein A/G magnetic beads ($n = 3$). After approximately 9 min, the beads have depleted the IgG level by 95%. Error bars represent 1 standard deviation about the mean. (B) Graph of mean relative fluorescence intensity (normalized to control) of FITC-IgG (solid, $n = 4$) and FITC-HSA (hatched, $n = 3$) as a function of one or two 10 min depletion step(s). The magnitude of the blank measurements was multiplied by 100 to illustrate the low background signal of on-chip fluorescent measurements. Error bars represent 1 standard deviation about the mean.

samples.⁴⁰ A mixture of HSA (0.5 mg/mL), IgG (2 mg/mL), and hemopexin (0.1 mg/mL) was used to represent a protein mixture composed of HAPs (HSA and IgG) and low-abundance proteins (hemopexin). Note that because of reagent availability and solubility issues, this mixture is not an identical match to the concentrations of these proteins in serum, but it does reflect the correct ratio of IgG to hemopexin (in serum, IgG is typically ~ 10 – $20\times$ more concentrated than hemopexin).

Figure 4 shows three representative MALDI-MS spectra for the protein mixture treated with (A) control (no depletion), (B) a single sample depletion step, and (C) two depletion steps. Four spectra were collected for each condition, and root-mean square noise (N_{RMS}) values were estimated from spectral regions without prominent peaks to determine signal-to-noise (S/N) ratios (Table 1). Initially, the low-abundant protein, hemopexin, produces very low relative signal intensity compared to the highly abundant species (IgG and HSA) in the protein mixture, prior to depletion, Figure 4A. The HSA is the most intense signal peak at approximately 152 ($S/N = 92.0$) while the singly and doubly charged intensities for IgG are 22 ($S/N = 23.9$) and 35 ($S/N = 22.0$), respectively. Conversely, the MALDI signal for hemopexin is quite low at approximately 13 ($S/N = 14.7$). The

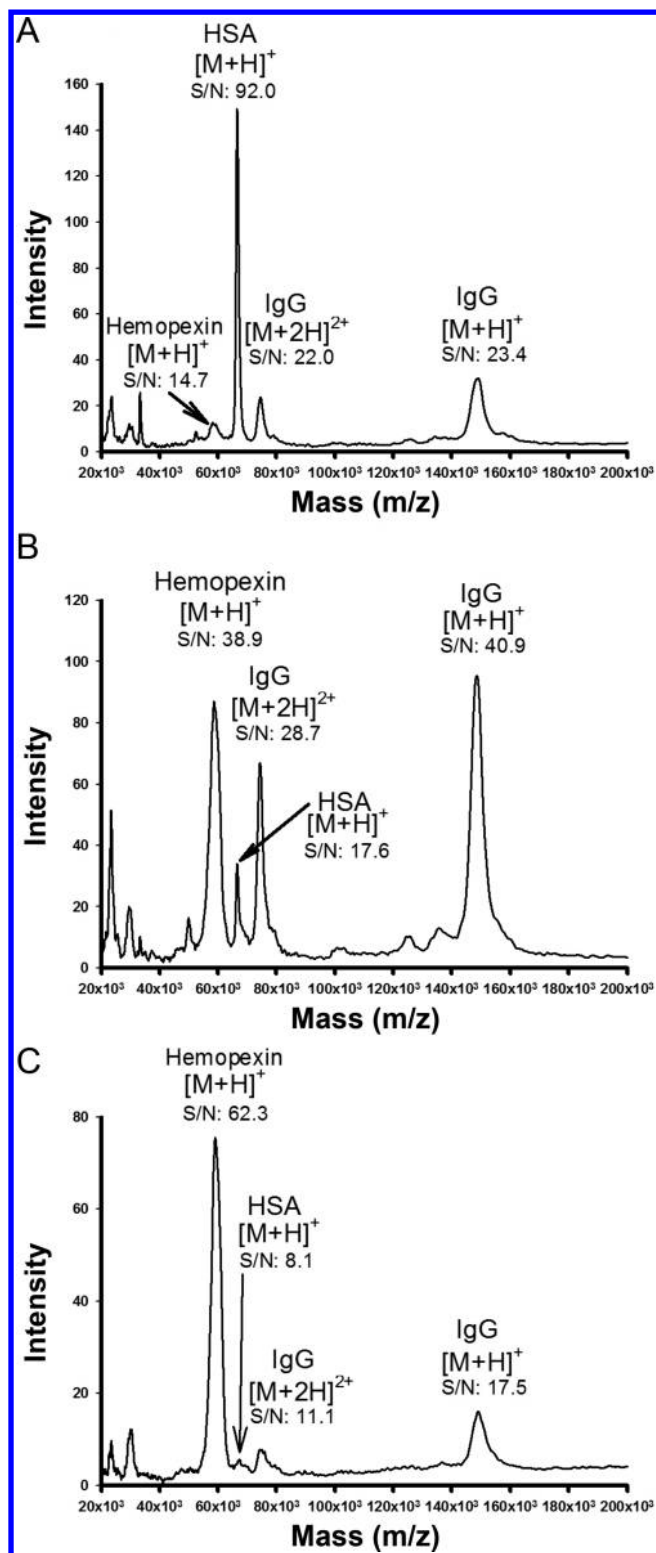


Figure 4. MALDI spectra of sample comprising HSA (0.5 mg/mL), IgG (2 mg/mL), and hemopexin (0.1 mg/mL). (A) Before depletion, (B) after single depletion, and (C) after double depletion.

low signal in the protein sample prior to extraction presumably results from charge competition/ion suppression due to the presence of the HAPs.⁴¹ The mixed protein sample was depleted using the DMF bead-based protocol (*vide supra*), and following a single depletion step, the hemopexin MALDI signal is increased 6.7 times to 87 ($S/N = 38.9$). Conversely, the HSA

Table 1. Comparison of S/N Ratios for Ion Intensities in MALDI-MS Spectra for the Control and Following a Single and Double Depletion, with the DMF/Magnetic Bead Platform

	analyte and S/N ratio			
	hemopexin ($M + H$) ⁺	HSA ($M + H$) ⁺	IgG ($M + 2H$) ²⁺	IgG ($M + H$) ⁺
control (no depletion)	14.65	92.04	21.98	23.35
single depletion 1	16.71	16.32	29.85	42.58
single depletion 2	38.81	17.61	28.66	40.90
single depletion 3	13.53	12.73	25.07	25.87
single depletion 4	22.21	15.78	23.81	28.63
mean single depletion	22.81	15.61	26.85	34.49
σ single depletion	11.25	2.07	2.87	8.47
double depletion 1	21.58	7.37	11.05	12.10
double depletion 2	40.72	10.66	14.54	17.94
double depletion 3	31.41	8.12	11.91	14.08
double depletion 4	62.25	8.14	11.05	17.45
mean double depletion	38.99	8.57	12.14	15.39
σ double depletion	17.37	1.44	1.65	2.78

signal is decreased by 5.2 times to 34 ($S/N = 17.6$) and now ranks as the fourth most intense peak behind IgG with intensities of 95 ($S/N = 40.9$) and 67 ($S/N = 28.7$), for +1 and +2 charge states, respectively (Figure 4B). Interestingly, the first depletion produces an increase in both the S/N ratio for the IgG and hemopexin, resulting from reduced ion suppression from the simplified matrix.

Following a double depletion, the MALDI signals for HSA and IgG are diminished to 5.5 ($S/N = 11.1$) for HSA, which corresponds to a 6.2 times reduction compared to the first depletion and a total reduction of 27.6 compared to the original sample, and IgG where the signal is reduced to 16 ($S/N = 17.5$) and 8.1 ($S/N = 11.1$) for the singly and doubly charged ions, respectively, with an overall average reduction of 2.5 for both IgG ions. Conversely, the hemopexin signal is now the most intense signal at 76 ($S/N = 62.3$) in the MALDI-MS spectrum with a signal enhancement of 5.6 and an improvement in signal-to-noise ratio of 4.2. Detailed results of S/N for each replicate are tabulated in Table 1.

A significant enhancement for hemopexin is observed when comparing the signal-to-noise (S/N) ratios of the peaks in the protein mixture before depletion and following a single and double depletion. Furthermore, the signal-to-noise ratios also point to the necessity of conducting a second depletion step as a significant protein concentration remains after the first step to limit the signal-to-noise enhancement. Similarly following protein depletion, a sample can be subjected to ESI-MS/MS. See the Supporting Information for the DMF-based protein depletion protocol with nanoliquid chromatography mass spectrometry.

CONCLUSION

We have demonstrated DMF separation of high-abundance and low-abundance proteins with antibody and bioaffinity protein-immobilized magnetic beads for a human plasma protein depletion application. Using this new method, protein depletion was successfully developed on DMF and is a powerful tool for rapid, efficient, and automated sample processing by achieving >95% depletion efficiency in as little as 10 min for multiple samples simultaneously (up to four on the current device). Current commercially available depletion methods for depletion of a single protein on columns require between 20 and 60 min for completion for a single sample. We eliminate the need for lengthy depletion protocols, high levels of sample dilution, or both. We propose that the new technique has great potential for biomarker identification.

ASSOCIATED CONTENT

Supporting Information

Additional information as noted in text. This material is available free of charge via the Internet at <http://pubs.acs.org/>.

AUTHOR INFORMATION

Corresponding Authors

*E-mail: Aaron.Wheeler@utoronto.ca.

*E-mail: Richard.Oleschuk@chem.queensu.ca.

Author Contributions

^{||}N.M. and B.S. contributed equally.

Notes

The authors declare no competing financial interest.

ACKNOWLEDGMENTS

We thank David McLeod for assistance with MALDI-MS and Dr. Jiayi Wang for assistance with LC-MS/MS. We also thank Dr. Mark Yang and Victor Lee for providing ideas and contributing to the experimental work. We thank the Natural Sciences and Engineering Research Council (NSERC) for financial support. N.M. and A.H.C.N thank NSERC for graduate fellowships, and A.R.W. thanks the Canada Research Chair (CRC) program for a CRC.

REFERENCES

- (1) Hanash, S. M.; Pitteri, S. J.; Faca, V. M. *Nature* **2008**, *452*, 571–579.
- (2) Anderson, N. L.; Anderson, N. G. *Mol. Cell. Proteomics* **2002**, *1*, 845–867.
- (3) Kratz, A.; Ferraro, M.; Sluss, P. M.; Lewandrowski, K. B. *N. Engl. J. Med.* **2004**, *351*, 1548–1563.
- (4) Mayne, J.; Starr, A. E.; Ning, Z.; Chen, R.; Chiang, C.-K.; Figeys, D. *Anal. Chem.* **2013**, *86*, 176–195.
- (5) Cao, Z.; Yende, S.; Kellum, J. A.; Robinson, R. A. *S. Int. J. Proteomics* **2013**, *2013*, 8.
- (6) Zeng, Z.; Hincapie, M.; Pitteri, S. J.; Hanash, S.; Schalkwijk, J.; Hogan, J. M.; Wang, H.; Hancock, W. S. *Anal. Chem.* **2011**, *83*, 4845–4854.
- (7) Stempfer, R.; Kubicek, M.; Lang, I. M.; Christa, N.; Gerner, C. *Electrophoresis* **2008**, *29*, 4316–4323.
- (8) Quero, C.; Colomé, N.; Prieto, M. R.; Carrascal, M.; Posada, M.; Gelpi, E.; Abian, J. *Proteomics* **2004**, *4*, 303–315.
- (9) Polaskova, V.; Kapur, A.; Khan, A.; Molloy, M. P.; Baker, M. S. *Electrophoresis* **2010**, *31*, 471–482.
- (10) Millionsi, R.; Tolin, S.; Puricelli, L.; Sbrignadello, S.; Fadini, G. P.; Tessari, P.; Arrigoni, G. *PLoS One* **2011**, *6*, No. e19603.

- (11) Govorukhina, N. I.; Keizer-Gunnink, A.; van der Zee, A. G. J.; de Jong, S.; de Bruijn, H. W. A.; Bischoff, R. J. *Chromatogr., A* **2003**, *1009*, 171–178.
- (12) Desrosiers, R.; Beaulieu, É.; Buchanan, M.; Béliveau, R. *Cell Biochem. Biophys.* **2007**, *49*, 182–195.
- (13) Ahmed, N.; Barker, G.; Oliva, K.; Garfin, D.; Talmadge, K.; Georgiou, H.; Quinn, M.; Rice, G. *Proteomics* **2003**, *3*, 1980–1987.
- (14) Chromy, B. A.; Gonzales, A. D.; Perkins, J.; Choi, M. W.; Corzett, M. H.; Chang, B. C.; Corzett, C. H.; McCutchen-Maloney, S. L. *J. Proteome Res.* **2004**, *3*, 1120–1127.
- (15) Guzman, N. A.; Blanc, T.; Phillips, T. M. *Electrophoresis* **2008**, *29*, 3259–3278.
- (16) Friedrich, D.; Please, C. P.; Melvin, T. J. *Chromatogr., B* **2012**, *910*, 163–171.
- (17) Malmstadt, N.; Yager, P.; Hoffman, A. S.; Stayton, P. S. *Anal. Chem.* **2003**, *75*, 2943–2949.
- (18) McKenzie, K. G.; Lafleur, L. K.; Lutz, B. R.; Yager, P. *Lab Chip* **2009**, *9*, 3543–3548.
- (19) Peoples, M. C.; Karnes, H. T. *J. Chromatogr., B* **2008**, *866*, 14–25.
- (20) Ng, A. H. C.; Uddayasankar, U.; Wheeler, A. *Anal. Bioanal. Chem.* **2010**, *397*, 991–1007.
- (21) Choi, K.; Ng, A. H. C.; Fobel, R.; Wheeler, A. R. *Annu. Rev. Anal. Chem.* **2012**, *5*, 413–440.
- (22) Cho, S. K.; Moon, H.; Chang-Jin, K. *J. Microelectromech. Syst.* **2003**, *12*, 70–80.
- (23) Shuford, C. M.; Hawkridge, A. M.; Burnett, J. C.; Muddiman, D. C. *Anal. Chem.* **2010**, *82*, 10179–10185.
- (24) Corrigan, L.; Jefferies, C.; Clive Lee, T.; Daly, J. *Proteomics* **2011**, *11*, 3415–3419.
- (25) Jebraill, M. J.; Wheeler, A. R. *Anal. Chem.* **2008**, *81*, 330–335.
- (26) Yang, H.; Mudrik, J. M.; Jebraill, M. J.; Wheeler, A. R. *Anal. Chem.* **2011**, *83*, 3824–3830.
- (27) Mudrik, J. M.; Dryden, M. D. M.; Lafreniere, N. M.; Wheeler, A. R. *Can. J. Chem.* **2014**, *92*, 179–185.
- (28) Wijethunga, P. A. L.; Nanayakkara, Y. S.; Kunchala, P.; Armstrong, D. W.; Moon, H. *Anal. Chem.* **2011**, *83*, 1658–1664.
- (29) Mousa, N. A.; Jebraill, M. J.; Yang, H.; Abdelgawad, M.; Metalnikov, P.; Chen, J.; Wheeler, A. R.; Casper, R. F. *Sci. Transl. Med.* **2009**, *1*, 1ra2.
- (30) Ng, A. H. C.; Choi, K.; Luoma, R. P.; Robinson, J. M.; Wheeler, A. R. *Anal. Chem.* **2012**, *84*, 8805–8812.
- (31) Choi, K.; Ng, A. H. C.; Fobel, R.; Chang-Yen, D. A.; Yarnell, L. E.; Pearson, E. L.; Oleksak, C. M.; Fischer, A. T.; Luoma, R. P.; Robinson, J. M.; Audet, J.; Wheeler, A. R. *Anal. Chem.* **2013**, *85*, 9638–9646.
- (32) Fobel, R.; Kirby, A. E.; Ng, A. H. C.; Farnood, R. R.; Wheeler, A. R. *Adv. Mater.* **2014**, *26*, 2838–2843.
- (33) Shamsi, M. H.; Choi, K.; Ng, A. H. C.; Wheeler, A. R. *Lab Chip* **2014**, *14*, 547–554.
- (34) Chatterjee, D.; Ytterberg, A. J.; Son, S. U.; Loo, J. A.; Garrell, R. L. *Anal. Chem.* **2010**, *82*, 2095–2101.
- (35) Luk, V. N.; Fiddes, L. K.; Luk, V. M.; Kumacheva, E.; Wheeler, A. R. *Proteomics* **2012**, *12*, 1310–1318.
- (36) Daley, A. B.; Xu, Z.; Oleschuk, R. D. *Anal. Chem.* **2011**, *83*, 1688–1695.
- (37) Fobel, R.; Fobel, C.; Wheeler, A. R. *Appl. Phys. Lett.* **2013**, *102*, 193513–193518.
- (38) Hadwen, B.; Broder, G. R.; Morganti, D.; Jacobs, A.; Brown, C.; Hector, J. R.; Kubota, Y.; Morgan, H. *Lab Chip* **2012**, *12*, 3305–3313.
- (39) Zolotarjova, N.; Martosella, J.; Nicol, G.; Bailey, J.; Boyes, B. E.; Barrett, W. C. *Proteomics* **2005**, *5*, 3304–3313.
- (40) Wong, M. Y. M.; Yu, K. O. Y.; Poon, T. C. W.; Ang, I. L.; Law, M.-K.; Chan, K. Y. W.; Ng, E. W. Y.; Ngai, S.-M.; Sung, J. J. Y.; Chan, H. L. Y. *Electrophoresis* **2010**, *31*, 1721–1730.
- (41) Sjö Dahl, J.; Kempka, M.; Hermansson, K.; Thorsén, A.; Roeraade, J. *Anal. Chem.* **2005**, *77*, 827–832.
- (42) Kullolli, M.; Warren, J.; Arampatzidou, M.; Pitteri, S. J. *J. Chromatogr., B* **2013**, *939*, 10–16.